Journal of Neuroscience Methods 238 (2014) 1–10

Contents lists available at ScienceDirect

Journal of Neuroscience Methods

journal homepage: www.elsevier.com/locate/jneumeth

An aerator for brain slice experiments in individual cell culture plate wells

David M. Dorris[a], Caitlin A. Hauser[a], Caitlin E. Minnehan[a], John Meitzen[a,b,*]

[a] Department of Biological Sciences, North Carolina State University, Raleigh, NC, USA
[b] W.M. Keck Center for Behavioral Biology, Center for Human Health and the Environment, and Center for Comparative Medicine and Translational Research, North Carolina State University, Raleigh, NC, USA

HIGHLIGHTS

- We have developed a new aerator designed to fit into a single well of a standard 24-well cell culture plate.
- The aerator keeps brain slices viable and stationary, and is inexpensive to produce.
- The aerator enables individual manipulation of living acute brain slices or potentially other tissues in low solution volumes.

GRAPHICAL ABSTRACT

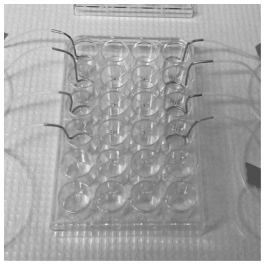

ARTICLE INFO

Article history:
Received 4 August 2014
Received in revised form
12 September 2014
Accepted 15 September 2014
Available online 22 September 2014

Keywords:
Brain slices
Aerator
Bubbler
24-Well culture plate
Oxygenation
Dorsal striatum
β-Adrenergic receptor
Caudate putamen

ABSTRACT

Background: Ex vivo acute living brain slices are a broadly employed and powerful experimental preparation. Most new technology regarding this tissue has involved the chamber used when performing electrophysiological experiments. Alternatively we instead focus on the creation of a simple, versatile aerator designed to allow maintenance and manipulation of acute brain slices and potentially other tissue in a multi-well cell culture plate.
New method: Here we present an easily manufactured aerator designed to fit into a 24-well cell culture plate. It features a nylon mesh and a single microhole to enable gas delivery without compromising tissue stability. The aerator is designed to be individually controlled, allowing both high throughput and single well experiments.
Results: The aerator was validated by testing material leach, dissolved oxygen delivery, brain slice viability and neuronal electrophysiology. Example experiments are also presented, including a test of whether β1-adrenergic receptor activation regulates gene expression in *ex vivo* dorsal striatum using qPCR.
Comparison with existing methods: Key differences include enhanced control over gas delivery to individual wells containing brain slices, decreased necessary volume, a sample restraint to reduce movement artifacts, the potential to be sterilized, the avoidance of materials that absorb water and small biological molecules, minimal production costs, and increased experimental throughput.
Conclusion: This new aerator is of high utility and will be useful for experiments involving brain slices and other potentially tissue samples in 24-well cell culture plates.
© 2014 Elsevier B.V. All rights reserved.

* Corresponding author at: Dept. of Biological Sciences, NC State University, 144 David Clark Labs, Campus Box 7617, Raleigh, NC 27695-7617, USA. Tel.: +1 919 515 4496; fax: +1 919 515 5327.
E-mail addresses: jemeitze@ncsu.edu, jmeitzen@gmail.com (J. Meitzen).

http://dx.doi.org/10.1016/j.jneumeth.2014.09.017
0165-0270/© 2014 Elsevier B.V. All rights reserved.

1. Introduction

Ex vivo acute living brain slices are a broadly employed and powerful experimental approach (Collingridge, 1995; Khurana and Li, 2013; Li and McIlwain, 1957; McIlwain et al., 1951; Yamamoto and McIlwain, 1966). Though most prominently associated with electrophysiological recordings, *ex vivo* brain slices have been used to test hypotheses across the entire continuum of neuroscience, using genetic, molecular, tissue culture, pharmacological, immunocytochemical, anatomical and many other approaches.

Brain slices are prepared by rapidly extracting the brain, exposing it to either warm or cold oxygenated artificial cerebrospinal fluid (ACSF), and sectioning the brain slices using a vibratome (Colbert, 2006; Huang and Uusisaari, 2013; Madison and Edson, 2001). Oxygenation is typically provided *via* carbogen gas (95% O_2/5% CO_2). After creation, brain slices are then usually maintained and then recorded from in one of two basic chamber types. The first chamber type submerges the tissue in relatively large volumes of oxygenated ACSF (Blake et al., 2007; Buskila et al., 2014; Croning and Haddad, 1998; Fujii and Toita, 1991; Hajos and Mody, 2009; Koerner and Cotman, 1983; Moyer and Brown, 1998; Nicoll and Alger, 1981; Sakmann et al., 1989; Thomas et al., 2013; Tominaga et al., 2000; White et al., 1978). The second is interface- or membrane-style chamber that places the tissue at the convergence/interface between oxygenated ACSF and humidified O_2/CO_2 (Dingledine et al., 1980; Haas et al., 1979; Hajos et al., 2009; Hill and Greenfield, 2011; Knowles, 1985; Li and McIlwain, 1957; Matthies et al., 1997; Tcheng and Gillette, 1996). The design and creation of brain slice chambers has been the subject of intense effort, especially regarding microfluidics (Ahrar et al., 2013; Huang et al., 2012; Mohammed et al., 2008; Scott et al., 2013; Thomas et al., 2013), and oxygen delivery (Blake et al., 2007; Choi et al., 2007; Hill and Greenfield, 2011; Oppegard et al., 2009; Rambani et al., 2009).

Less attention has been directed toward designing chambers for *ex vivo* manipulation of individual brain slices for the purposes other than electrophysiology, and the maintenance and storage of brain slices, especially in low volumes of ACSF. Here we aim to fill this gap by presenting a new aerator designed to allow easy manipulation and maintenance of brain slices and potentially other tissues in low volumes in multi-well cell culture plates. Multi-well cell culture plates, and in particular 24-well plates were chosen given their versatility and prevalence.

We first describe in detail the design and operation of the aerator. We then validate the device using inductively coupled plasma optical emission spectrometry (ICP-OES) to test for material leach, dissolved oxygen measurements to test for gas delivery, infrared-differential interference contrast (IR-DIC) microscopy and tetrazolium chloride (TTC) staining to test brain slice viability, and electrophysiology to test neuronal physiology. We then present example applications, including immunocytochemistry and a test of whether β1-adrenergic receptor activation in *ex vivo* dorsal striatum regulates gene expression using real-time polymerase chain reaction (qPCR). We conclude that new aerator is of high utility and will be useful for experiments involving brain slices and other potentially other tissue samples in 24-well cell culture plates.

2. Materials and methods

2.1. Aerator design

The aerator is constructed from 18 ga stainless steel tubing (Part no. HTX-18R-30, 304 SS Hypo Tube 18 ga. Regular Wall, Component Supply Company, Florida, http://www.componentsupplycompany.com/), with a nylon mesh (Cat no. 64-0198, Warner Instruments, Connecticut, https://www.warneronline.com/) used to restrain brain slices (or potentially other tissues) (Fig. 1A). At the bottom is a 15 mm inner diameter loop with a single 0.343 mm hole in the top of the loop, opposite where the end of the tube meets a 90 degree turn in the tube. The open end is crimped. The shaft runs approximately 20 mm to where it meets another 90 degree bend. After this bend, the shaft runs approximately 10 mm where it remains open for gas line attachment. While the bottom loop can be manufactured with or without a nylon mesh, we find that the mesh is useful for restraining samples at the bottom of the well. The mesh is currently constructed of nylon because of its relative inertness and long use with brain slices. However, the mesh could potential be constructed of other materials such as polyester or polypropylene.

Once constructed, the bubbler is attached to a gas line controlled by a manifold and placed in a culture well (Fig. 1B and C). 2 mL of solution in the well was found to be optimal and was used in all the experiments reported here, however, the well could also hold 1 or 3 mL of solution. 2 mL was chosen for the working volume as increased cavitation was observed with ≤1 mL volume, and 3 mL increased the risk of spillover and aerosol contamination of other wells. Once in solution the gas (in our case, 95% O_2/5% CO_2) was turned on using the manifold. We found that the microhole in the bottom loop of the aerator provided adequate oxygenation with minimal sample disruption, and thus we did not place a tubing crimp to regulate gas flow. Additionally, when multiple aerators are in use (Fig. 1D), gas exposure was more rigorously controlled by using a common manifold than individual crimps.

We find that this basic design met our requirements for the aerator. First, the aerator needed to fit snugly into the well of a 24 well cell culture plate. This was achieved *via* the 15 mm diameter rounded bottom. Second, the brain slice must be kept stationary. This was achieved *via* the nylon mesh affixed to the top of the rounded bottom, and the single microhole used for gas delivery. Third, the aerator needed to be individually controlled in exclusion to all other wells. This criterion was met by creating an aerator with individually-controlled operation. Fourth, we wanted the aerator to be made out of a material that can potential be sterilized, that does not absorb water or small molecules, and with minimal release of endocrine disruptors. We thus considered three broad materials: plastic, glass, and finally stainless steel. Plastic was our initial choice, due to the relative ease of manufacture and the potential possibility of construction using 3-D printers. However, many of the plastics employed for 3-D printer construction are toxic to neurons (Hyde et al., 2014). Our primary consideration was polydimethlysiloxane (PDMS), which has been employed in other multi-well culture plate aerators and brain slice chambers (Blake et al., 2007; Oppegard et al., 2009, 2010). PDMS has many advantages for aeration, however, PDMS is known to absorb water and small biological molecules (Heo et al., 2007; Mukhopadhyay, 2007; Randall and Doyle, 2005; Roman et al., 2005). This makes it unsuitable for many experiments involving living tissue, and especially brain slices. These considerations, along with the potential release of additional endocrine disruptors (Gore and Patisaul, 2010) led us to consider other materials, although we note that the presented schematic could still potentially be used with 3-D printers. The second material we evaluated was glass. However, we quickly ran into severe challenges with manufacturing. That, along with the possibility of leached materials (Doremus, 1994; Kay, 2004; Nunamaker et al., 2013), led us to our current material, stainless steel. We found stainless steel to be advantageous in that it was relatively easy to manipulate, was already commonly used in many biomedical applications, was relatively inexpensive and was able to be sterilized. One potential drawback to stainless steel is like glass and some plastics is the potential for the leaching of heavy metals in solution. We directly tested this using ICP-OES, and aerators actively employed in the laboratory between 6 and 12 months.

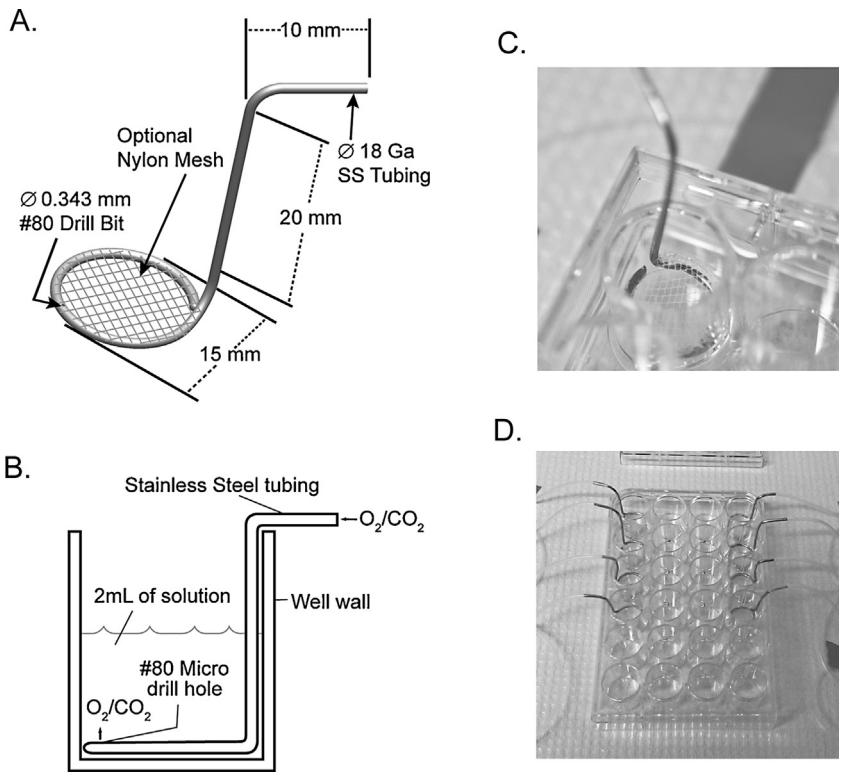

Fig. 1. An aerator for *ex vivo* manipulation of individual living brain slices in 24-well cell culture plates. (A) Overhead schematic of the aerator, including an optional mesh to stabilize brain slices. (B) Side schematic of the aerator, placed in a well of a 24-well culture plate. (C) Overhead picture of an aerator placed in a 24-well culture plate. In this case the aerator is attached to tubing to deliver gas. (D) An array of aerators prepared for an experiment. All aerators are placed in individual wells, and attached to tubing to deliver gas. The tubing is attached to a manifold in order to control gas flow. In an experiment, one or two living brain slices would be placed in each aerated well with 2 mL of ACSF.

Table 1
Metal concentrations.

Metal	Minimum detection limit (μg/L)	Control (μg/L)	Aerator (μg/L)	Statistics (t, P)
Chromium (Cr)	1.0	1.0 ± 0, (0)	1.0 ± 0, (0)	N/A
Iron (Fe)	2.0	2.0 ± 0, (0)	4.0 ± 2.1, (1)	1.00, 0.36
Nickel (Ni)	2.0	2.0 ± 0, (0)	2.5 ± 0.5, (1)	1.00, 0.36
Zinc (Zn)	1.0	1.9 ± 0.6, (2)	2.3 ± 0.4, (4)	0.62, 0.56

Note: Numbers in parentheses indicate number of samples with detectable metal levels. For statistical analysis and calculations of means and SEM, the minimum detection limit was used for samples with no detectable element concentration. Values are mean ± SEM. $n = 4$ samples for each element. N/A: Not applicable.

Little evidence of leaching was found when procedures typical of our experiments are used (Section 3.1 and Table 1). We do note that care must be taken to visually inspect the aerator before use, and that different grades/batches of stainless steel could present different material leach profiles. Thus, we conclude that while stainless steel is not a perfect material, it offers the best combination of functionality along with known and well-understood limitations.

2.2. Aerator manufacture

Aerator manufacture is straightforward and followed a plan created *via* a computer-aided design package (Fig. 1A; SolidWorks, Dassault Systemes, Massachusetts). First an 80 mm length of 18 ga stainless steel tubing was cut and one end crimped. The crimped end was then fitted around a 13 mm diameter mounted cylinder. The tube was then wrapped around the cylinder and the crimped end placed next to the shaft. A 90 degree bend was then introduced where the shaft met the crimped end. 20 mm from the initial 90 degree bend, a second 90 degree bend was then introduced into the tube. Any excess tubing as then trimmed to create the 10 mm neck. At this point a single 0.343 mm microhole was drilled on the side of the loop opposite the crimped end, using a no. 80 drill bit connected to a Dremel tool. Nylon mesh was then affixed using cyanoacrylate glue (Krazy Glue) and allowed to dry for at least 1 h. This relatively simple manufacturing process enabled a short build time for the aerator. This met our fifth goal for the device, that the aerator be easy and inexpensively manufactured with little specialized equipment.

2.3. Aerator operation

Operation was likewise simple. While it is possible to control each aerator with an individual tubing crimp, in practice we found that this was difficult to control when using more than one aerator. We thus used tubing to attach all aerators to manifolds controlled with a single switch. This allowed rapid and synchronous operation of the aerators. After use, aerators were washed with dH_2O and 70% ethanol unless they were disposed of due to drug exposure or other compromising event.

2.4. ICP-optical emission spectroscopy (ICP-OES)

Measurements of iron (Fe), Zinc (Zn), Nickel (Ni), and Chromium (Cr) were made with an Optima 8000 ICP-OES Spectrometer (Perkin

Elmer) by the NC State University Environmental and Agricultural Testing Service (http://www.soil.ncsu.edu/services/asl/). Data was collected using a Meinhard nebulizer and a cyclonic spray chamber to achieve the highest sensitivity. Before data collection, the injector tube, torch, and spray chamber were acid washed, and new tubing was installed. 3 mL of dH_2O was placed in 16 individual wells of a 24 well culture plate for 1 h, 8 wells contained aerators and 8 did not (control). At the end of the hour, dH_2O was extracted from each well and pooled with one other well from the same experimental group to meet minimum volume requirements. Thus the number of analyzed samples per group was 4. Detection limits varied for each element (Fe, 2.0 μg/L; Cr, 1.0 μg/L; Ni, 2.0 μg/L; Zn, 1.0 μg/L). Calibration checks were made for each element, and linearity was verified using a 0 to 10 μg/L concentration curve. Samples were run in a single assay. As an additional control, two different wavelengths were used to analyze the same sample set for Zn concentration. Variability in Zn concentration detected by the two different wavelengths was 1.0%, indicating excellent precision. For statistical analysis and calculations of means the minimum detection limit was used for samples with no detectable element concentration.

2.5. Oxygen concentration measurements

Dissolved oxygen concentration measurements were made with a Vernier Dissolved Oxygen Probe (DO-BTA) and Vernier Lab Pro Software (Vernier, Beaverton, OR) following previous work from other laboratories (Noradoun and Cheng, 2005).

2.6. Animals

All animal protocols were approved by Institutional Animal Care and Use Committee at North Carolina State University and carried out in accordance with the National Institute of Health Guide for the Care and Use of Laboratory Animals (NIH Publications no. 80-23). Sprague-Dawley CD IGS rats were born from timed-pregnant females purchased from Charles River (Raleigh, NC). Animals were housed with their littermates and dam until weaning on day 21, and then with same-sex littermates. All cages were washed polysulfone (BPA-free) and were filled with bedding manufactured from virgin hardwood chips (Beta Chip, NEPCO, Warrensburg, NY). Rooms were temperature, humidity and light-controlled (23 °C, 40% humidity, 12 h light:12 h darkness cycle). Soy protein-free rodent chow (2020X, Teklad, Madison, WI, USA) and glass-bottle provided water were available *ad libitum.*

2.7. Brain slice preparation

Methods for preparing brain slices were adapted from previous studies (Meitzen et al., 2009; Wissman et al., 2011). Rats were deeply anesthetized with isoflurane and killed by decapitation. The brain was dissected rapidly into ice-cold, oxygenated sucrose artificial CSF (sACSF) containing (in mM): 75 sucrose, 1.25 NaH_2PO_4, 3 $MgCl_2$, 0.5 $CaCl_2$, 2.4 Na pyruvate, 1.3 ascorbic acid from Sigma-Aldrich, St. Louis, MO, and 75 NaCl, 25 $NaHCO_3$, 15 dextrose, 2 KCl from Fisher, Pittsburg, PA; osmolarity 295–305 mOsm, pH 7.2–7.4. Coronal brain slices (300 μm) were prepared using a vibratome and then incubated in regular ACSF containing (in mM): 126 NaCl, 26 $NaHCO_3$, 10 dextrose, 3 KCl, 1.25 NaH_2PO_4, 1 $MgCl_2$, 2 $CaCl_2$, 295–305 mOsm, pH 7.2–7.4) for 30 min at 35 °C, and at least 30 min at room temperature (21–23 °C) in a large volume bath holder. Slices were stored submerged in room temperature oxygenated ACSF for up to 6 h after sectioning in either a standard storage container or in a 24 well plate cell culture well with the aerator described here.

2.8. Electrophysiology and IR-DIC imaging

After resting for ≥1 h after sectioning, and for 1–6 h in an individual well with aerator, slices were placed in a Zeiss Axioscope equipped with IR-DIC optics, a Dage IR-1000 video camera, and 10X and 40X lenses with optical zoom. Slices were superfused with oxygenated ACSF heated to 27 ± 1 °C. Whole-cell patch-clamp recordings were made from two visually-identified medium spiny neurons (MSNs) in the dorsal striatum using glass electrodes (4–8 MΩ) containing (in mM): 115 K D-gluconate, 8 NaCl, 2 EGTA, 2 $MgCl_2$, 2 MgATP, 0.3 NaGTP, 10 phosphocreatine from Sigma-Aldrich and 10 HEPES from Fisher, 285 mOsm, pH 7.2–7.4). Signals were amplified, filtered (2 kHz), and digitized (10 kHz) with a MultiClamp 700B amplifier attached to a Digidata 1550 system and a personal computer using pClamp 10 software. Membrane potentials were not corrected for a calculated liquid junction potential of −13.5 mV. Using previously described procedures (Farries et al., 2005; Meitzen et al., 2009), recordings were made in current clamp to confirm MSN identify and to assess electrophysiological properties.

2.9. 2,3,5-Triphenyltetrazolium chloride (TTC) staining

TTC staining was used to assess brain slice health using protocols adapted from previously published experiments (Bederson et al., 1986; Llano et al., 2014; Watson et al., 1994). For each experiment, 4 brain slices of dorsal striatum were prepared from each animal ($n = 4$ males) and allowed to rest 1 h after sectioning. Slices were then equally divided into 4 experimental groups: (1) 1 h, slices were placed into individual wells of a 24 well cell culture plate and exposed for 1 h to oxygenated ACSF using the aerator described in this paper. (2) 2 h, slices were placed into individual wells of a 24 well cell culture plate and exposed for 2 h to oxygenated ACSF using the aerator. (3) Negative control (−). Slices were placed into individual wells of a 24 well cell culture plate and exposed for 2 h to non-oxygenated, dextrose-free ACSF containing 500 μM kainic acid to induce cell death (K0250, Sigma). (4) Positive control (+). Slices were placed in TTC solution immediately after rest. Following experimental manipulation, slices were placed for 30 min in freshly prepared and filtered 2% TTC (T-8877; Sigma) solution in either oxygenated ACSF or non-oxygenated, dextrose-free ACSF on an orbital shaker. Slices were then washed 3 times for 30 s each in phosphate-buffered saline (PBS). Slices were fixed using ice-cold 4% paraformaldehyde (Electron Microscopy Sciences) and 4 mM EGTA in PBS overnight at 4 °C. Slices were washed three times for 5 min each in PBS, and then cryoprotected using 15% sucrose for 30 min and then 30% sucrose in PBS overnight at 4 °C. For quantification, brain slices were embedded in gelatin (1 g gelatin + 1 g sucrose per 10 mL dH_2O), and cut cross-sectionally (90 degrees to the original cutting plane; to measure TTC staining in both the exterior and interior of the slice) in 50 μm increments using a freezing microtome. Slices were mounted using Citifluor (Ted Pella). Micrographs were acquired using a Leica DM5000B system. Images were imported into ImageJ (http://rsbweb.nih.gov/ij), and inverted using the "image inverter" macro. Mean gray values were then measured and background subtracted.

2.10. Immunocytochemistry

Protocols for immunocytochemistry were adapted from those described previously (Karadottir and Attwell, 2006; Meitzen et al., 2013a). Brain slices were placed in an individual well with aerator for 2 h. Slices were fixed using ice-cold 4% paraformaldehyde (Electron Microscopy Sciences) in PBS containing 4 mM

EGTA for 1 h. Tissue was washed three times in PBS for 10 min each, and placed in 0.1% Triton X-100 (VWR Scientific), 1% BSA and 2% goat serum (Jackson ImmunoResearch) overnight at 4 °C. Tissue was washed three times in PBS, and then incubated at room temperature for 24 h in PBS containing 1% BSA, 2% goat serum, and a monoclonal antibody directed against serine 133-phosphorylated cAMP response element-binding protein (pCREB, 1:1000; catalog no. 05-667, Upstate Biotechnology), and a polyclonal antibody targeting microtubule-associated protein 2 (MAP2) (1:1000; catalog no. AB5622; Calbiochem). Tissue was washed three times in PBS and then incubated for 4 h in PBS with 1% BSA, 2% goat serum, and Alexa Fluor 488-conjugated anti-rabbit and Alexa Fluor 635-conjugated anti-mouse (1:1000, A11008 and A31574; Invitrogen) secondary antibodies for visualization of MAP2 and pCREB, respectively. Tissue was washed three times in PBS and mounted using Citifluor (Ted Pella). Fluorescent micrographs were acquired using a Leica DM5500Q confocal system using Leica LAS AF (version 1.9.0; Leica).

2.11. PCR

For each experiment, 8 brain slices of dorsal striatum were prepared from each animal ($n = 4$ for isoproterenol studies; $n = 7$ for xamoterol studies; all adult males) and allowed to rest 1 h after sectioning. Slices were then placed in individual wells of a 24-well cell culture plate and aerated using the aerator. 4 slices were exposed for 1 h to either 1 μM Xamoterol (a β1-adrenergic receptor partial agonist which is specific for the β1-adrenergic receptor at the employed concentration; Tocris) (Abraham et al., 2008; Luchowska et al., 2009) or 10 μM isoproterenol (a pan-specific β1- and β2-adrenergic receptor agonist) (Meitzen et al., 2011). 4 other slices were exposed to vehicle solution. Slices were then placed in RNAlater (Qiagen), and incubated overnight at 4 °C, then overnight at −20 °C before archive at −80 °C. Once all tissue was collected, slices were thawed and mRNA extracted, pooled, and reverse transcribed using standard kits (RNAeasy Mini or Midi Kit or QuantiTect Reverse Transcription Kit as appropriate; QIAGEN).qPCR was performed using standard protocols (Meitzen et al., 2013b). qPCR amplification was performed using an Applied Biosystems 7300 PCR machine using SYBR Green Select Master Mix (Life Technologies, 4472908). Threshold values were calculated and then standardized to the ribosome-related gene *rpl13a* ($2\hat{}\Delta\Delta c(t)$ method), and control values (Drug/Control). The thermal cycling program used was a pre-incubation step at 95 °C for 5 min, followed by at least 45 cycles consisting of a 10 s denaturing step at 95 °C, annealing step for 10 s at 60 °C, an extension step for 10 s at 72 °C, and a measurement of fluorescent intensity. At the end of each cycling program, a melting curve was run. PCR for individual cDNA samples was performed in triplicate, and overall experiments were repeated twice.

The upper and lower primer sequences used were as follows: *rpl13a* (GenBank accession number NM_173340; Meitzen et al., 2011): 5′-TGCTGCCGCACAAGACCAAA-3′ and 5′-AACTTTCTGGTAGGCTTCAGCCGC-3′; *penk* (GenBank accession number NM_017139.1; Lindenbach et al., 2011): 5′-CATGAAACCG-CCATACCTCT-3′ and 5′-AAAATCTGGGAGACCTGCAA-3′; *pdyn* (Genbank accession number NM_019374.3): 5′-AGCTTGCCTCC-TTGTGATCC-3′ and 5′-TTGGTCAGTTCCGTGTAGCC-3′; *fos* (GenBank accession number NM_022197.2; (Meitzen et al., 2011): 5′-TATAGGTAGTGCAGCTGGGAGTGC-3′ and 5′-TGCCAGATGTGGACC-TGTCTGGTT-3′; *tac1* (designed to amplify all four transcript variants, Genbank accession numbers NM_001124770.1, NM_012666.2, NM_001124769.1, NM_001124768.1): 5′-GAATCA-GCATCCCGTTTGCC-3′ and 5′-CGGAGCCCTTTGAGCATCTT-3′.

2.12. Statistics

Experiments were analyzed using one way ANOVAs with Tukey's Multiple Comparison tests, or *t* tests as appropriate (Prism version 5.00; GraphPad Software, La Jolla, CA). *P* values <0.05 were considered *a priori* as significant. Data are presented as mean ± SEM.

3. Results

3.1. Aerator material validation

As discussed in Section 2.1, Design Considerations, a number of different materials were considered for aerator construction. After considering the strengths and weaknesses of each material, stainless steel was chosen for its durability, malleability, the ability to be sterilized, the lack of endocrine disruptor release, and its relative inertness regarding water and small biological molecules. One possible drawback to stainless steel is the possibility of heavy metal leaching in solution. To test this we placed dH_2O into wells in a 24 well culture plate containing or not containing aerators for a final sample size of $n = 4$ per group. To better simulate experimental conditions, all aerators had been actively used in the laboratory between 6 and 12 months. The concentrations of chromium (Cr), iron (Fe), Nickel (Ni), and Zinc (Zn) were then tested using ICP-OES. Overall, metal concentrations were low to non-detectable across elements (Table 1), and for statistical analysis and calculations of means the minimum detection limit was used for samples with no detectable element concentration. No chromium was detected in any sample. Iron was below detectable limits in all control samples, and 3 aerator samples. No difference in iron concentration was detected between groups ($t_{(6)} = 1.0$; $P = 0.3559$). Similarly, nickel was below detectable limits in all control samples, and 3 aerator samples. No difference in nickel concentration was detected between groups ($t_{(6)} = 1.0$; $P = 0.3559$). Zinc was below the detectable limit in 2 control samples. No difference in zinc concentration was detected between groups ($t_{(6)} = 0.6194$; $P = 0.5584$), and overall zinc concentrations are equivalent or below those typically encountered in similar preparations (Bresink et al., 1996; Frederickson et al., 2006; Kay, 2004; Nunamaker et al., 2013). These results indicate that minimal leaching of metals occurs from the aerators, validating their use with biological samples.

3.2. Aerator oxygenation validation

To be effective an aerator must be able to provide sufficient oxygenation. We first tested this by assembling an array of 12 aerators in a 24 well culture plate and dividing them into three experimental groups. All wells contained 2 mL of ACSF. Two groups(both $n = 4$) were supplied with 95% oxygen/5% carbon dioxide, in order to oxygenate the solution using the gas mixture most commonly employed for acute brain slice experiments, and to help maintain pH for accurate dissolved oxygen measurements. These groups were allowed to aerate for 1 or 2 h, respectively. For a negative control, one group of aerators was not supplied with gas ($n = 4$; "−"). For a positive control, measurements were also taken from traditional large volume submerged bath slice chambers holding 200 mL of ACSF and aerated using a large aquarium bubbler ($n = 4$; "+"). Use of the aerator effectively oxygenated the solution (Fig. 2A; $F_{(3,15)} = 374$; $P < 0.0001$). Interestingly, no differences were detected in oxygenation levels between the single well aerators and the standard slice holder, indicating that saturation was achieved in all groups.

This experiment is useful in establishing the long-term effectiveness of the aerator, but provides little information regarding

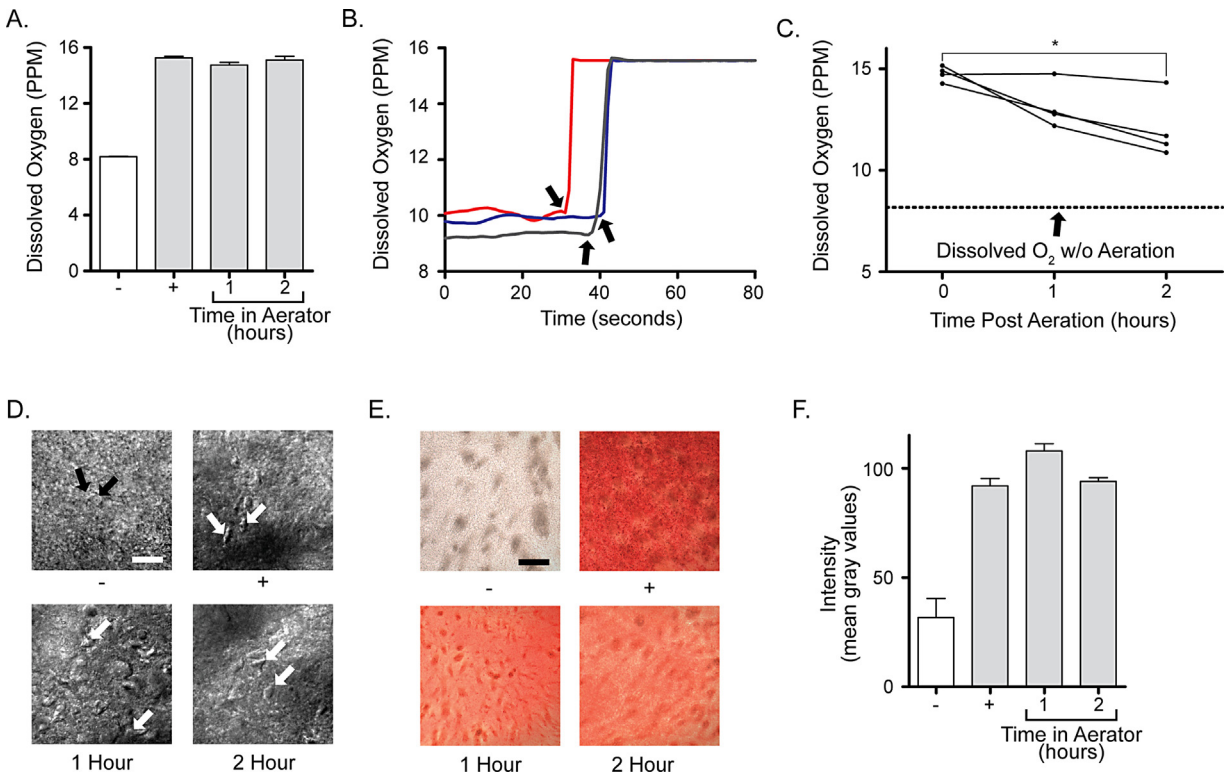

Fig. 2. Aerator oxygenation and biological validation. (A) The aerator effectively oxygenates ACSF placed in the well. Dissolved oxygen levels in wells exposed for 1 and 2 h to carbogen gas do not differ from those measured in the positive control (+), a large volume submerged brain slice chamber. All oxygenated groups show significantly increased dissolved oxygen compared to the negative control (−), a well exposed only to atmospheric oxygen and containing an un-activated aerator. ACSF and carbogen gas were used for all tests because they are most relevant to actual experimental conditions. (B) Aerators rapidly oxygenate 2 mL of ACSF in a well. All three aerators tested increase dissolved oxygen levels within 2 s after exposure to carbogen gas. In this panel different colors indicate individual aerators/wells. Arrows indicate oxygen onset. (C) Dissolved oxygen levels remain elevated post-aeration. 2 mL ACSF was placed in 4 wells and oxygenated for 2 min. Dissolved oxygen levels were then measured at 0, 1 and 2 h post-oxygenation. Dissolved oxygen levels remained elevated 1 h after initial exposure, and were decreased at 2 h. For reference, dissolved oxygen levels without aeration are indicated. (D) IR-DIC visualization of brain slices of adult rat dorsal striatum indicates that brain slices incubated with the aerator for 1 or 2 h (1 h; 2 h) contain healthy neurons comparable to those from the positive control (+), a traditional large volume bath slice holder. The negative control (−) are neurons intentionally killed using un-oxygenated, dextrose-free ACSF containing kainic acid. Scale bar is 25 μm. White arrows indicate living neurons, and dark arrows indicate dead neurons. Dark and light striations in the micrograph are typical of adult dorsal striatum. (E) TTC staining indicates that brain slices incubated with the aerator (1 h; 2 h) are healthy and comparable to those from the positive control (+), a traditional large volume bath slice holder. The negative control (−) are brain slices intentionally killed using un-oxygenated, dextrose-free ACSF containing kainic acid. Scale bar is 200 μm. Dark striations in the micrograph are typical of adult dorsal striatum. (F) Quantification of TTC staining. TTC staining in slices incubated with the aerator for 1 or 2 h are indistinguishable from those incubated in a traditional large volume bath slice holder (+). The 1 h, 2 h, and positive control all show elevated TTC staining compared to the negative control (−). Different colors indicate statistical significance; complete statistical information is in Section 3. (For interpretation of the references to color in this figure legend, the reader is referred to the web version of this article.)

how quickly the aerator can saturate ACSF. To assess this, we assembled three aerators and continually measured dissolved oxygen levels in 2 mL of ACSF in wells before and during oxygenation with 95% oxygen/5% carbon dioxide (Fig. 2B). All three wells reached saturation within 2 s of gas exposure (1.7 ± 0.3 PPM), indicating a rapid increase in dissolved oxygen concentration. In contrast to this rapid increase in dissolved oxygen concentration, wells remained oxygenated for hours after an initial 2 min exposure to gas (Fig. 2 C; $F_{(2,11)} = 9.8$; $P = 0.130$). Indeed, dissolved oxygen concentration did not significantly decrease until 2 h after initial oxygen exposure ($P < 0.05$). Collectively, these data indicate that the aerator robustly and rapidly increases dissolved oxygen exposure in the culture plate well, and that the well retains dissolved oxygen levels for hours after a short initial exposure.

3.3. Aerator biological validation

To be useful for brain slice experiments, an aerator must not only be able to effectively oxygenate culture wells but must also be able to keep acute living brain slices viable, preferably for hours. Thus our next step was to assess whether brain slices placed in a culture well with an aerator remained healthy. Our first experiment to test this was to again assemble an array of 12 aerators in a 24 well culture plate and dividing them into three experimental groups. Similar to the experiment depicted in Fig. 2A, living brain slices of rat dorsal striatum were placed in culture wells oxygenated by an aerator for 1 h ($n = 4$), or 2 h ($n = 4$), or intentionally killed by being placed in dextrose-free ACSF containing kainic acid and no active oxygenation ($n = 4$, negative control, "−"). A fourth group of brain slices were kept in a large volume bath slice holder (200 mL ACSF) and used as a positive control ($n = 4$, "+"). Following experimental treatment, neurons in the brain slices were visualized using IR-DIC microscopy (Fig. 2D). As expected, no living neurons were found in the negative control, and abundant living neurons were found in the positive control. The appearance and relative number of living neurons were visually indistinguishable between the 1 h and 2 h experimental groups and the positive control. This experiment indicates that individual neurons remain healthy and numerous in wells containing aerators.

We next sought to quantify the overall health of the brain slices. To do this we employed TTC staining, which is a mitochondrial marker indicative of living neural tissue (Figu. 2E) (Bederson et al., 1986; Llano et al., 2014; Watson et al., 1994). The same experimental groups were employed as in the experiment depicted in Fig. 2D ($n = 6$ per group). As expected, brain slices of dorsal striatum subjected to the negative control were white, indicating cell death, and

brain slices from the positive control, 1 h, and 2 h groups were red and indistinguishable from one another, indicating healthy tissue (Fig. 2F, $F_{(3,23)} = 43.16$; $P < 0.0001$; $P > 0.05$ between positive control "+" and 1 and 2 h groups; note that images were inverted for quantification, hence the "mean gray value" units). These data indicate that brain slices remain viable up to 2 h in aerated wells, and that the general level of health is directly comparable to that of traditional large volume submerged storage chambers.

In some experimental applications acute brain slices are incubated for longer time periods than 2 h. One possibility is that the low volumes used with this method may probe problematic for longer term incubation given that acute brain slices slowly release active biological compounds into the surrounding ACSF. To assess this, we made living brain slices of rat dorsal striatum, divided them into three experimental groups ($n = 3$ for each group), and exposed them to each experimental manipulation for 6 h. The first group of brain slices was placed into a large volume bath slice holder (500 mL ACSF). The second group of brain slices was placed into culture wells containing ACSF that was oxygenated with an aerator and not changed. The third group of brain slices was placed into culture wells containing ACSF that was oxygenated with an aerator and changed every 2 h. Following the 6 h experimental treatment, neurons in the brain slices were visualized using IR-DIC microscopy (Fig. 3). Living neurons and dead neurons were found in all three experimental groups. Qualitatively, the number of living neurons as well as the overall appearance of the brain slice appeared increased in brain slices oxygenated by the aerator and receiving a solution change every 2 h. This experiment indicates that living neurons can be found in brain slices in wells oxygenated with the aerator for a longer time period. Additionally, this experiment suggests that periodically changing the ACSF within the well during longer incubations may be beneficial for brain slice viability.

3.4. Example experimental applications

After establishing that the aerator effectively maintains brain slice health, we then performed a series of experiments designed to test various potential applications of the aerator. These include electrophysiology, immunocytochemistry, and qPCR. Regarding electrophysiology, we made brain slices of adult rat dorsal striatum, allowed them to rest for 1 h, and then incubated them in an aerated well for an additional hour. Using a blunt plastic transfer pipette, we then transferred the brain slice to a perfusion slice chamber (PC-R, Siskiyou) attached to a visualized whole-cell patch clamp rig. Striatal medium spiny neurons were identified from the medium sized, rounded soma, and electrophysiological properties recorded (Fig. 4A). Medium spiny neurons exhibited normal properties, including the presence of a slow ramping subthreshold depolarization in response to low-magnitude positive current injections, a hyperpolarized resting potential, inward rectification, and prominent spike afterhyperpolarization (Belleau and Warren, 2000; O'Donnell and Grace, 1993; Wilson and Groves, 1981). This indicates that the aerator does not grossly confound electrophysiological properties, and that brain slices may be maintained as either control or experimental groups in the aerated well for up to 2 h.

We next assessed the usefulness of the aerator for immunocytochemistry. Brain slices of adult rat dorsal striatum were again prepared and allowed to rest for 1 h, after which they were placed in an aerated well for 2 h. We then performed immunocytochemistry for microtubule-associated protein 2 (MAP2), a cytoskeletal marker useful for visualizing neurons, and phosphorylated cAMP response element binding protein (CREB), a transcription factor that is a commonly used experimental endpoint (Fig. 4B) (Carlezon et al., 2005; Meitzen et al., 2012). Immunocytochemistry appeared normal, supporting the conclusion that the aerator will be useful for incubating and manipulating brain slices prior to pharmacological and immunocytochemistry procedures.

Finally, we tested whether the aerator would be useful for experiments involving qPCR. Specifically, we tested whether activation of β1-adrenergic receptors induces changes in striatal mRNA expression by exposing brain slices to β1-adrenergic receptor agonists and then measuring changes in the cDNA of genes using qPCR. These genes include *fos, penk, tac*, and *pdyn*, all implicated in striatal neural plasticity and/or L-DOPA-induced dyskinesia (Konradi et al., 1994; Lindenbach et al., 2011). This experiment is of interest given the lack of information regarding the role of β1-adrenergic receptors in striatal function, and their potential application as a target for new L-DOPA-induced dyskinesia and drug addiction therapies (Barnum et al., 2012; Hara et al., 2010; Lindenbach et al., 2011; Meitzen et al., 2011; Ostock et al., 2014; Rommelfanger and Weinshenker, 2007; Schmidt and Weinshenker, 2014). Thus, we again made brain slices of dorsal striatum from adult rats. Slices were allowed to rest for 1 h, and were then placed in aerated wells for 1 h. Slices from each animal were divided into two groups, control or drug exposed. In the first experiment, slices were exposed to vehicle control or isoproterenol, a panspecific β1- and β2-adrenergic receptor agonist ($n = 4$ per group). Exposure to isoproterenol decreased *fos* expression (Fig. 4C; $t_{(3)} = 6.6$; $P = 0.0072$). In the second experiment, a drug specific for the β1-adrenergic receptor was employed. Slices were exposed to vehicle control or xamoterol, a β1-adrenergic receptor partial agonist ($n = 7$ per group). Exposure to xamoterol decreased *fos, penk* and *tac* expression (Fig. 4C; $t_{(6)} = 3.8$; $P = 0.0091$; $t_{(6)} = 3.4$; $P = 0.0144$; $t_{(5)} = 10.54$; $P = 0.0001$). We note that one data point in the *tac* group failed the outlier test and was excluded from analysis (value: 3.2). If the data point is included *tac* expression is not significantly decreased, although 6 of 7 data points indicate decreased expression (0.63 ± 0.43; $t_{(6)} = 0.85$; $P > 0.05$). Exposure to xamoterol had no effect on *pdyn* expression (Fig. 4C; $t_{(6)} = 1.1$; $P > 0.05$). These experiments indicate that activation of β1-adrenergic receptors in the dorsal striatum induces changes in select gene expression related to neural plasticity and L-DOPA-induced dyskinesia. More broadly, this experiment provides an example of the utility of the single well aerator for targeted manipulation of brain slices.

4. Discussion

Here we present a new aerator designed for use with acute brain slices in 24-well cell culture plates. Significantly, this device offers control of gas delivery to individual wells in the culture plate, the use of small volumes of solution which may be advantageous for pharmacological experiments, a nylon mesh and a single microhole for gas delivery to enable sample stability, the potential to be sterilized, the avoidance of materials that absorb water and small biological molecules, minimal production costs, and potentially increased experimental throughput.

In addition to presenting schematics, a discussion of aerator design, and instructions for aerator manufacture and operation, we have validated the aerator in three different spheres. We first tested for material leach using ICP-OES. We found little evidence for significant metal release given the experimental parameters employed. However there is no perfect material for aerator construction. Given our laboratory's research emphasis, we avoid whenever possible plastics such as PDMS that may absorb water or small biological molecules (Heo et al., 2007; Mukhopadhyay, 2007; Randall and Doyle, 2005; Roman et al., 2005), and have instead opted for stainless steel, at least for now.

We next validated the aerator's effectiveness in oxygenating relevant volumes of solution. This was necessary given the microhole employed for gas delivery. The aerator was found to rapidly increase and maintain dissolved oxygen concentrations. In

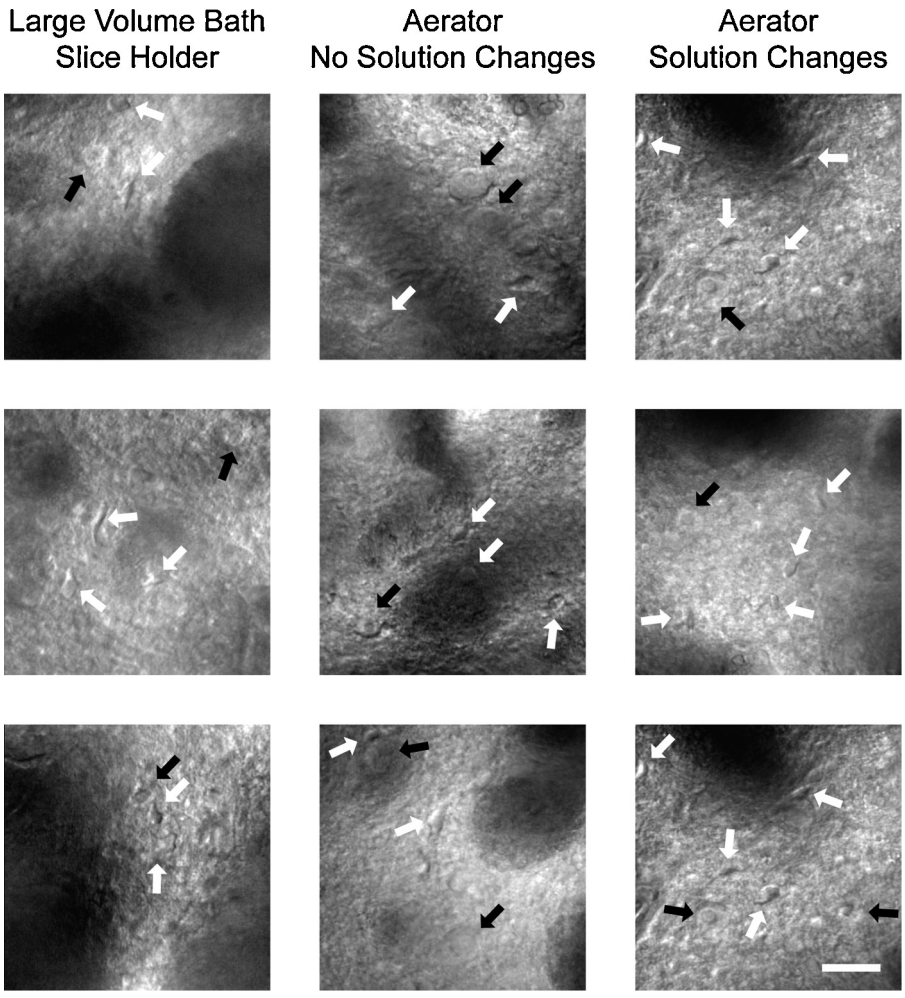

Fig. 3. Aerator biological validation with increased incubation duration. IR-DIC visualization of brain slices of adult rat dorsal striatum indicates that brain slices incubated with the aerator for 6 h contain healthy neurons comparable to those incubated in a traditional large volume slice holder and that periodic solution changes may increase slice viability. Left column: IR-DIC images of brain slices incubated in a large volume bath slice holder for 6 h. Middle column: IR-DIC images of brain slices incubated with the aerator for 6 h with no ACSF solution changes. Right column: IR-DIC images of brain slices incubated with the aerator for 6 h with ACSF solution changes every 2 h. Scale bar is 25 μm. White arrows indicate living neurons, and dark arrows indicate dead neurons. Dark and light striations in the micrograph are typical of adult rat dorsal striatum.

addition, it was discovered that the small volume of ACSF employed remained oxygenated for over an hour after gas delivery was ended. After establishing that the aerator provided effective oxygenation, we then validated the use of the aerator with acute brain slices. Using IR-DIC microscopy, TTC staining and electrophysiology we found that brain slices remained viable and that neuronal electrophysiology remained normal. In addition to the electrophysiological recordings we then present two possible applications:

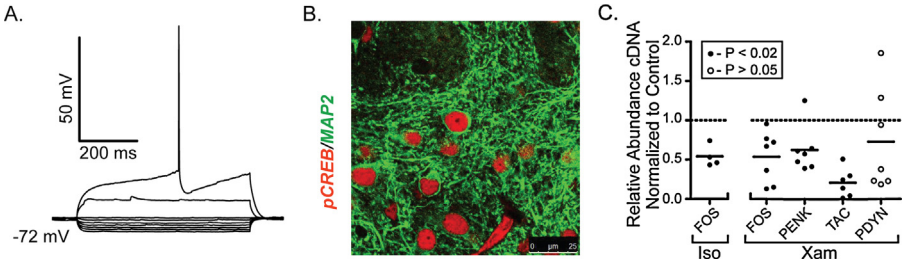

Fig. 4. Example experimental applications. (A) Electrophysiology. An acute brain slice of adult rat dorsal striatum was prepared, allowed to rest for 1 h, incubated for an additional hour in an aerated culture well, and then placed on a whole-cell patch clamp rig. A striatal medium spiny neuron was visually identified, whole-cell patch clamped in current clamp configuration and electrophysiological properties recorded. Electrophysiological properties were typical of those of this neuron type, including the presence of a slow ramping subthreshold depolarization in response to low-magnitude positive current injections, a hyperpolarized resting potential, inward rectification, and prominent spike afterhyperpolarization. (B) Immunocytochemistry. Example confocal image of a dorsal striatum brain slice incubated in an aerated well for 2 h. Neurons were immunolabeled with the neuron-specific cytoskeletal protein MAP2 (green) and phosphorylated CREB (pCREB; red). Scale bar is 25 μm. Dark patches are typical of adult dorsal striatum. C) qPCR. Experiment 1 (left): exposure to the panspecific β1- and β2-adrenergic receptor agonist isoproterenol for 1 h in the aerated culture well reduced *fos* expression in dorsal striatum brain slices. Experiment 2 (right): Exposure to the specific β1-adrenerigic receptor agonist xamoterol for 1 h in the aerated culture well reduced *fox*, *penk*, and *tac* expression in dorsal striatum brain slices. Exposure to xamoterol had no effect on *pdyn* expression. (For interpretation of the references to color in this figure legend, the reader is referred to the web version of this article.)

increased ease of immunocytochemistry of brain slices, and pharmacological manipulation of receptors to study changes in gene expression. In particular, we tested whether β1-adrenergic receptor activation changed the expression of genes related to striatal function and L-DOPA-induced dyskinesia in dorsal striatum. We found that β1-adrenergic receptor activation changed the expression of *fos, penk* and *tac*, building upon previous studies in primary striatal neuron cell culture and *in vivo* dorsal striatum (Hara et al., 2010; Lindenbach et al., 2011; Meitzen et al., 2011).

An additional experimental option may be the use of this aerator with cultured or long term maintenance of brain or other tissue. In that case we note that the aerator can be sterilized given its stainless steel construction, although a material other than nylon would mostly likely need to be employed for the webbing, if it is used at all. It would also be possible to modify the aerator for use in other types of multi-well plates. In that case the diameter of the cylinder employed in manufacture would be adjusted for the size of the cell culture plate well.

5. Conclusion

In conclusion, the new aerator design presented here is easily manufactured, offers high utility and simplicity, and will be useful for experiments involving living brain slices and other potentially tissue samples in multi-well cell culture plates.

Acknowledgments

This work was supported by NC State University Startup Funds (JM) and an HHMI Undergraduate Science Education grant (CH, CM; PI: Dr. Damien Shea). We thank Kim Hutchison of the NCSU EATS Facility, Colleen Brannen, Dr. Robert Grossfeld, Dr. Jinyan Cao, and Dr. Heather Patisaul for their assistance.

References

Abraham PA, Xing G, Zhang L, Yu EZ, Post R, Gamble EH. Li H. beta1- and beta2-adrenoceptor induced synaptic facilitation in rat basolateral amygdala. Brain Res 2008;1209:65–73.
Ahrar S, Nguyen TV, Shi Y, Ikrar T, Xu X, Hui EE. Optical stimulation and imaging of functional brain circuitry in a segmented laminar flow chamber. Lab Chip 2013;13:536–41.
Barnum CJ, Bhide N, Lindenbach D, Surrena MA, Goldenberg AA, Tignor S, et al. Effects of noradrenergic denervation on L-DOPA-induced dyskinesia and its treatment by alpha- and beta-adrenergic receptor antagonists in hemiparkinsonian rats. Pharmacol Biochem Behav 2012;100:607–15.
Bederson JB, Pitts LH, Germano SM, Nishimura MC, Davis RL, Bartkowski HM. Evaluation of 2,3,5-triphenyltetrazolium chloride as a stain for detection and quantification of experimental cerebral infarction in rats. Stroke 1986;17:1304–8 (a journal of cerebral circulation).
Belleau ML, Warren RA. Postnatal development of electrophysiological properties of nucleus accumbens neurons. J Neurophysiol 2000;84:2204–16.
Blake AJ, Pearce TM, Rao NS, Johnson SM, Williams JC. Multilayer PDMS microfluidic chamber for controlling brain slice microenvironment. Lab Chip 2007;7:842–9.
Bresink I, Ebert B, Parsons CG, Mutschler E. Zinc changes AMPA receptor properties: results of binding studies and patch clamp recordings. Neuropharmacology 1996;35:503–9.
Buskila Y, Breen PP, Tapson J, van Schaik A, Barton M, Morley JW. Extending the viability of acute brain slices. Sci Rep 2014;4:5309.
Carlezon WA Jr, Duman RS, Nestler EJ. The many faces of CREB. Trends Neurosci 2005;28:436–45.
Choi Y, McClain MA, LaPlaca MC, Frazier AB, Allen MG. Three dimensional MEMS microfluidic perfusion system for thick brain slice cultures. Biomed Microdevices 2007;9:7–13.
Colbert CM. Preparation of cortical brain slices for electrophysiological recording. Methods Mol Biol 2006;337:117–25 (Clifton, NJ).
Collingridge GL. The brain slice preparation: a tribute to the pioneer Henry McIlwain. J Neurosci Methods 1995;59:5–9.
Croning MD, Haddad GG. Comparison of brain slice chamber designs for investigations of oxygen deprivation in vitro. J Neurosci Methods 1998;81:103–11.
Dingledine R, Dodd J, Kelly JS. The in vitro brain slice as a useful neurophysiological preparation for intracellular recording. J Neurosci Methods 1980;2:323–62.
Doremus R. Glass science. New York: Wiley-Interscience; 1994. p. 352.
Farries MA, Meitzen J, Perkel DJ. Electrophysiological properties of neurons in the basal ganglia of the domestic chick: conservation and divergence in the evolution of the avian basal ganglia. J Neurophysiol 2005;94:454–67.
Frederickson CJ, Giblin LJ 3rd, Balaji RV, Masalha R, Frederickson CJ, Zeng Y, et al. Synaptic release of zinc from brain slices: factors governing release, imaging, and accurate calculation of concentration. J Neurosci Methods 2006;154:19–29.
Fujii T, Toita K. A method for simultaneous recording of electrical activities and spectrophotometric signals from brain slice preparations in vitro. Pflugers Arch 1991;419:205–8 (European journal of physiology).
Gore AC, Patisaul HB. Neuroendocrine disruption: historical roots, current progress, questions for the future. Front Neuroendocrinol 2010;31:395–9.
Haas HL, Schaerer B, Vosmansky M. A simple perfusion chamber for the study of nervous tissue slices in vitro. J Neurosci Methods 1979;1:323–5.
Hajos N, Ellender TJ, Zemankovics R, Mann EO, Exley R, Cragg SJ, Freund TF, Paulsen O. Maintaining network activity in submerged hippocampal slices: importance of oxygen supply. Eur J Neurosci 2009;29:319–27.
Hajos N, Mody I. Establishing a physiological environment for visualized in vitro brain slice recordings by increasing oxygen supply and modifying aCSF content. J Neurosci Methods 2009;183:107–13.
Hara M, Fukui R, Hieda E, Kuroiwa M, Bateup HS, Kano T, et al. Role of adrenoceptors in the regulation of dopamine/DARPP-32 signaling in neostriatal neurons. J Neurochem 2010;113:1046–59.
Heo YS, Cabrera LM, Song JW, Futai N, Tung YC, Smith GD, et al. Characterization and resolution of evaporation-mediated osmolality shifts that constrain microfluidic cell culture in poly(dimethylsiloxane) devices. Anal Chem 2007;79:1126–34.
Hill MR, Greenfield SA. The membrane chamber: a new type of in vitro recording chamber. J Neurosci Methods 2011;195:15–23.
Huang S, Uusisaari MY. Physiological temperature during brain slicing enhances the quality of acute slice preparations. Front Cell Neurosci 2013;7:48.
Huang Y, Williams JC, Johnson SM. Brain slice on a chip: opportunities and challenges of applying microfluidic technology to intact tissues. Lab Chip 2012;12:2103–17.
Hyde J, MacNicol M, Odle A, Garcia-Rill E. The use of three-dimensional printing to produce in vitro slice chambers. J Neurosci Methods 2014 [Epub ahead of Print].
Karadottir R, Attwell D. Combining patch-clamping of cells in brain slices with immunocytochemical labeling to define cell type and developmental stage. Nat Protoc 2006;1:1977–86.
Kay AR. Detecting and minimizing zinc contamination in physiological solutions. BMC Physiol 2004;4:4.
Khurana S, Li WK. Baptisms of fire or death knells for acute-slice physiology in the age of 'omics' and light? Rev Neurosci 2013;24:527–36.
Knowles WD. A portable in vitro brain slice chamber. J Neurosci Methods 1985;14:187–92.
Koerner JF, Cotman CW. A microperfusion chamber for brain slice pharmacology. J Neurosci Methods 1983;7:243–51.
Konradi C, Cole RL, Heckers S, Hyman SE. Amphetamine regulates gene expression in rat striatum via transcription factor CREB. J Neurosci 1994;14:5623–34.
Li CL, McIlwain H. Maintenance of resting membrane potentials in slices of mammalian cerebral cortex and other tissues in vitro. J Physiol 1957;139:178–90.
Lindenbach D, Ostock CY, Eskow Jaunarajs KL, Dupre KB, Barnum CJ, Bhide N<Et-AL>. Behavioral and cellular modulation of L-DOPA-induced dyskinesia by beta-adrenoceptor blockade in the 6-hydroxydopamine-lesioned rat. J Pharmacol Exp Ther 2011;337:755–65.
Llano DA, Slater BJ, Lesicko AM, Stebbings KA. An auditory colliculothalamocortical brain slice preparation in mouse. J Neurophysiol 2014;111:197–207.
Luchowska E, Kloc R, Olajossy B, Wnuk S, Wielosz M, Owe-Larsson B, et al. Beta-adrenergic enhancement of brain kynurenic acid production mediated via cAMP-related protein kinase A signaling. Prog Neuro-psychopharmacol Biol Psychiatry 2009;33:519–29.
Madison DV, Edson EB, et al. Preparation of hippocampal brain slices. In: Crawley Jacqueline N, editor. Current protocols in neuroscience/editorial board. New York: Wiley; 2001 (Chapter 6: Unit 6.4).
Matthies H, Schulz S, Thiemann W, Siemer H, Schmidt H, Krug M<Et-AL>. Design of a multiple slice interface chamber and application for resolving the temporal pattern of CREB phosphorylation in hippocampal long-term potentiation. J Neurosci Methods 1997;78:173–9.
McIlwain H, Buchel L, Cheshire JD. The inorganic phosphate and phosphocreatine of Brain especially during metabolism in vitro. Biochem J 1951;48:12–20.
Meitzen J, Grove DD, Mermelstein PG. The organizational and aromatization hypotheses apply to rapid, nonclassical hormone action: neonatal masculinization eliminates rapid estradiol action in female hippocampal neurons. Endocrinology 2012;153:4616–21.
Meitzen J, Luoma J, Stern C, Mermelsten PG. ß1-Adrenergic receptors activate two distinct signaling pathways in striatal neurons. J Neurochem 2011;116:984–95.
Meitzen J, Luoma JI, Boulware MI, Hedges VL, Peterson BM, Tuomela K, et al. Palmitoylation of estrogen receptors is essential for neuronal membrane signaling. Endocrinology 2013a;154:4293–304.
Meitzen J, Perry AN, Westenbroek C, Hedges VL, Becker JB, Mermelstein PG. Enhanced striatal β1-adrenergic receptor expression following hormone loss in adulthood is programmed by both early sexual differentiation and puberty: a study of humans and rats. Endocrinology 2013b;154:1820–31.
Meitzen J, Weaver AL, Brenowitz EA, Perkel DJ. Plastic and stable electrophysiological properties of adult avian forebrain song-control neurons across changing breeding conditions. J Neurosci 2009;29:6558–67.
Mohammed JS, Caicedo HH, Fall CP, Eddington DT. Microfluidic add-on for standard electrophysiology chambers. Lab Chip 2008;8:1048–55.

Moyer JR Jr, Brown TH. Methods for whole-cell recording from visually preselected neurons of perirhinal cortex in brain slices from young and aging rats. J Neurosci Methods 1998;86:35–54.
Mukhopadhyay R. When PDMS isn't the best. What are its weaknesses, and which other polymers can researchers add to their toolboxes? Anal Chem 2007;79:3248–53.
Nicoll RA, Alger BE. A simple chamber for recording from submerged brain slices. J Neurosci Methods 1981;4:153–6.
Noradoun CE, Cheng IF. EDTA degradation induced by oxygen activation in a zerovalent iron/air/water system. Environ Sci Technol 2005;39:7158–63.
Nunamaker EA, Otto KJ, Artwohl JE, Fortman JD. Leaching of heavy metals from water bottle components into the drinking water of rodents. J Am Assoc Lab Anim Sci: JAALAS 2013;52:22–7.
O'Donnell P, Grace AA. Physiological and morphological properties of accumbens core and shell neurons recorded in vitro. Synapse (New York, NY) 1993;13:135–60.
Oppegard SC, Blake AJ, Williams JC, Eddington DT. Precise control over the oxygen conditions within the Boyden chamber using a microfabricated insert. Lab Chip 2010;10:2366–73.
Oppegard SC, Nam KH, Carr JR, Skaalure SC, Eddington DT. Modulating temporal and spatial oxygenation over adherent cellular cultures. PLoS One 2009;4:e6891.
Ostock CY, Lindenbach D, Goldenberg AA, Kampton E, Bishop C. Effects of noradrenergic denervation by anti-DBH-saporin on behavioral responsivity to L-DOPA in the hemi-parkinsonian rat. Behav Brain Res 2014;270:75–85.
Rambani K, Vukasinovic J, Glezer A, Potter SM. Culturing thick brain slices: an interstitial 3D microperfusion system for enhanced viability. J Neurosci Methods 2009;180:243–54.
Randall GC, Doyle PS. Permeation-driven flow in poly(dimethylsiloxane) microfluidic devices. Proc Nat Acad Sci USA 2005;102:10813–8.
Roman GT, Hlaus T, Bass KJ, Seelhammer TG, Culbertson CT. Sol-gel modified poly(dimethylsiloxane) microfluidic devices with high electroosmotic mobilities and hydrophilic channel wall characteristics. Anal Chem 2005;77:1414–22.
Rommelfanger KS, Weinshenker D. Norepinephrine the redheaded stepchild of Parkinson's disease. Biochem Pharmacol 2007;74:177–90.
Sakmann B, Edwards F, Konnerth A, Takahashi T. Patch clamp techniques used for studying synaptic transmission in slices of mammalian brain. Q J Exp Physiol (Cambridge, England) 1989;74:1107–18.
Schmidt KT, Weinshenker D. Adrenaline rush: the role of adrenergic receptors in stimulant-induced behaviors. Mol Pharmacol 2014;85:640–50.
Scott A, Weir K, Easton C, Huynh W, Moody WJ, Folch A. A microfluidic microelectrode array for simultaneous electrophysiology, chemical stimulation, and imaging of brain slices. Lab Chip 2013;13:527–35.
Tcheng TK, Gillette MU. A novel carbon fiber bundle microelectrode and modified brain slice chamber for recording long-term multiunit activity from brain slices. J Neurosci Methods 1996;69:163–9.
Thomas MG, Covington JA, Wall MJ. A chamber for the perfusion of in vitro tissue with multiple solutions. J Neurophysiol 2013;110:269–77.
Tominaga T, Tominaga Y, Yamada H, Matsumoto G, Ichikawa M. Quantification of optical signals with electrophysiological signals in neural activities of Di-4-ANEPPS stained rat hippocampal slices. J Neurosci Methods 2000;102:11–23.
Watson GB, Lopez OT, Charles VD, Lanthorn TH. Assessment of long-term effects of transient anoxia on metabolic activity of rat hippocampal slices using triphenyltetrazolium chloride. J Neurosci Methods 1994;53:203–8.
White WF, Nadler JV, Cotman CW. A perfusion chamber for the study of CNS physiology and pharmacology in vitro. Brain Res 1978;152:591–6.
Wilson CJ, Groves PM. Spontaneous firing patterns of identified spiny neurons in the rat neostriatum. Brain Res 1981;220:67–80.
Wissman AM, McCollum AF, Huang GZ, Nikrodhanond AA, Woolley CS. Sex differences and effects of cocaine on excitatory synapses in the nucleus accumbens. Neuropharmacology 2011;61:217–27.
Yamamoto C, McIlwain H. Electrical activities in thin sections from the mammalian brain maintained in chemically-defined media in vitro. J Neurochem 1966;13:1333–43.